

CERN-TH/98-77
LPTHE-Orsay/98-11
IFUM/613-FT
LNF-98/008(P)
hep-ph/9803400

THE p_T SPECTRUM IN HEAVY-FLAVOUR HADROPRODUCTION

Matteo Cacciari¹

LPTHE, Université Paris-Sud, Orsay, France

Mario Greco

Dipartimento di Fisica E. Amaldi, Università di Roma Tre
and INFN, Laboratori Nazionali di Frascati, Italy

Paolo Nason²

CERN, TH Division, Geneva, Switzerland

Abstract

We consider the transverse-momentum distribution of heavy flavours in hadronic collisions. We present a formalism in which large transverse-momentum logarithms are resummed at the next-to-leading level, and mass effects are included exactly up to order α_s^3 , so as to retain predictivity at both small and large transverse momenta. As an example, we apply our formalism to b production at the Tevatron.

CERN-TH/98-77

March 20, 1998

¹Work supported by an EC TMR Marie Curie fellowship under contract No. ERBFM-BICT972126.

²On leave of absence from INFN, Milan, Italy

1 Introduction

Next-to-leading order calculations of heavy-flavour production have been available for a long time [1, 2, 3, 4]. These calculations exploit the fact that the mass of the heavy quark acts as an infrared cutoff on collinear singularities, and thus the cross section has a power expansion in the strong coupling constant, evaluated at a renormalization scale near the heavy-quark mass m . This approach is appropriate when the heavy-quark mass is the only relevant mass scale of the problem, and it is bound to fail when the transverse momentum of the heavy quark is much larger than its mass. In fact, in this case, one cannot pinpoint a single characteristic scale in the problem, since all momenta between m and p_T are equally involved. It turns out that, whether we choose the renormalization scale μ_R and the factorization scale μ_F of order m or of order p_T , large logarithms of the ratio p_T/m arise to all orders in the perturbative expansion, and spoil its convergence. The logarithmic structure of the perturbative expansion for the inclusive transverse-momentum distribution can be classified in terms of the form $\alpha_s^2(\alpha_s \log p_T/m)^k$ (which we call leading-logarithmic terms, or LL), plus terms of the form $\alpha_s^3(\alpha_s \log p_T/m)^k$ (next-to-leading logarithmic terms, or NLL), and so on.

An early attempt to deal with this problem was described in ref. [2], where an order- α_s^3 calculation of the p_T spectrum was presented. There, in order to deal with the logarithmically enhanced terms, the following approach was adopted: the scales μ_R and μ_F were chosen of the order of p_T , and the first neglected LL terms (that is to say, the terms of order $\alpha_s^2(\alpha_s \log p_T/m)^2$) were estimated. Their value was used as an error on the resulting cross section. This procedure, of course, ends up giving large errors for very large p_T , but a reasonable range of p_T can be accessed in this way.

Alternatively, the whole tower of LL and NLL corrections can be computed using the fragmentation-function formalism [5]. This approach has however the drawback that it is essentially a “massless” formalism, in the sense that all contributions to the cross section that are suppressed by powers of m/p_T are not included. Although these corrections must be small when $\log p_T/m$ is large, it is however never clear at what values of p_T they can really be neglected.

The purpose of this work is to construct a formalism in which the fixed-order and the fragmentation-function approaches are merged, in the following sense:

- All terms of order α_s^2 and α_s^3 are included exactly, including mass effects.

- All terms of order $\alpha_s^2 \alpha_s^k \log^k p_T/m$ and $\alpha_s^3 \alpha_s^k \log^k p_T/m$ are also included exactly.

To be more specific, let us write schematically the result of the NLO calculation of the hadronic cross section as

$$\frac{d\sigma}{dp_T^2} = A(m)\alpha_s^2 + B(m)\alpha_s^3 + \mathcal{O}(\alpha_s^4). \quad (1.1)$$

The explicit dependence upon the centre-of-mass energy E_{cm} , p_T and μ is not indicated, and $\alpha_s = \alpha_s(\mu)$. The NLL resummed calculation is given by

$$\begin{aligned} \frac{d\sigma}{dp_T^2} &= \alpha_s^2 \sum_{i=0}^{\infty} a_i (\alpha_s \log \mu/m)^i + \alpha_s^3 \sum_{i=0}^{\infty} b_i (\alpha_s \log \mu/m)^i \\ &+ \mathcal{O}(\alpha_s^4 (\alpha_s \log \mu/m)^i) + \mathcal{O}(\alpha_s^2 \times \text{PST}), \end{aligned} \quad (1.2)$$

where PST stands for terms suppressed, in the large- p_T limit, by powers of m/p_T , irrespectively of further powers of logarithms and of α_s . The coefficients a_i and b_i depend upon E_{cm} , p_T and μ . If $\mu \approx p_T$, they do not contain large logarithms of the order of $\log p_T/m$. The only large logarithms are the ones explicitly indicated. Our approach combines the results of eqs. (1.1) and (1.2), giving

$$\begin{aligned} \frac{d\sigma}{dp_T^2} &= A(m)\alpha_s^2 + B(m)\alpha_s^3 + \\ &\left(\alpha_s^2 \sum_{i=2}^{\infty} a_i (\alpha_s \log \mu/m)^i + \alpha_s^3 \sum_{i=1}^{\infty} b_i (\alpha_s \log \mu/m)^i \right) \times G(m, p_T) \\ &+ \mathcal{O}(\alpha_s^4 (\alpha_s \log \mu/m)^i) + \mathcal{O}(\alpha_s^4 \times \text{PST}), \end{aligned} \quad (1.3)$$

where the function $G(m, p_T)$ is quite arbitrary, except that it must approach 1 when $m/p_T \rightarrow 0$, up to terms suppressed by powers of m/p_T . Observe that the sums now start from $i = 2$ and $i = 1$, respectively, in order to avoid double counting. Thus, this formalism contains all the information coming from the fixed-order NLO calculation, and from the NLL resummed calculation. The arbitrariness in the G factor arises from the fact that we do not know the structure of power-suppressed terms in the NLL resummed calculation.

In the present work, we adopt the shortest path for obtaining the correct answer, making use of an already existing computation of the $\mathcal{O}(\alpha_s^3)$ cross section (*fixed-order approach*, or FO) and of already available computer codes to evaluate the resummed cross section in the massless limit (*resummed approach*, or RS).

In order to carry out our program, it is important that both the RS and the FO approaches are expressed in the same renormalization scheme. The commonly used FO approach uses a renormalization and factorization scheme in which the heavy flavour is treated as heavy. Thus, if, for example, we are dealing with bottom production, we use α_s of 4 light flavours as our running coupling constant, and the appropriate structure functions should not include the bottom quark in the evolution. The RS approach, on the other hand, also includes the heavy flavour as an active, light degree of freedom. This problem can be easily overcome by a simple change of scheme in the FO calculation. Section 3 contains the details of this procedure.

Once this is done, the FO calculation matches exactly the terms up to order α_s^3 in the resummed approach, in the limit where power-suppressed mass terms are negligible. In order to subtract from the RS result the fixed-order terms already present in the FO, we must provide an approximation to the latter where only logarithmic mass terms are retained. We will call this “massless limit” FOM0. In the simplified notation of eqs. (1.1) and (1.2) we have

$$A(m) = a_0 + \text{PST}, \quad B(m) = a_1 \log \mu/m + b_0 + \text{PST}, \quad (1.4)$$

and the FOM0 approximation is given by

$$\frac{d\sigma}{dp_T^2} = a_0 \alpha_s^2 + (a_1 \log \mu/m + b_0) \alpha_s^3 + \mathcal{O}(\alpha_s^2 \times \text{PST}). \quad (1.5)$$

Our final result will be given by

$$\text{FONLL} = \text{FO} + (\text{RS} - \text{FOM0}) \times G(m, p_T). \quad (1.6)$$

The notation FONLL stands for fixed-order plus next-to-leading logs. Formula (1.6) is our practical implementation of eq. (1.3).

An alternative approach to the problem has been given in ref. [6], using an extension of a method developed for the computation of heavy-flavour effects in deep-inelastic scattering [7]. There, however, NLL terms are not fully included. We will comment on this approach in due time.

The paper is organized as follows. We first review in sect. 2 the resummed approach, and in sect. 3 we describe the procedure to adopt in order to translate the FO result from a scheme with $n_f - 1$ light flavours to a scheme with n_f light flavours. In sect. 4 we give a few details concerning the calculation of the massless

limit of the FO calculation. In sect. 5 we check the matching between the FOM0 and the RS calculation, by explicitly verifying that the difference RS-FOM0 is of order α_s^4 . In sect. 6 we examine the size of power-suppressed effects in order to understand at which value of m/p_T the massless approach gives a sensible approximation to the massive calculation. The function $G(m, p_T)$ will be chosen on the basis of the considerations given in this section. In sect. 7 we describe a simplified version of our FONLL calculation, in which only LL resummation is adopted. In sect. 8 we describe an alternative choice for the factorization scheme for the fragmentation function. In sect. 9 we describe our full result, for the case of bottom production at the Tevatron. Finally, in sect. 10 we give our conclusions.

When computing specific cross sections, we will always use the parton densities set CTEQ3M, which implements a correct treatment of the bottom parton density. Since this set uses a mass of 5 GeV for the bottom quark, we will also employ the same value for consistency.

2 Review of the resummation formalism

Essential ingredients for the resummation formalism are the perturbative fragmentation functions [8] for the parton i to go into the heavy quark h , $D_i(x, \mu)$, where i runs over all the light partons (e.g. the light quarks and antiquarks, and the gluon) plus the heavy quark and antiquark. These fragmentation functions satisfy the standard Altarelli–Parisi evolution equations, and their initial values at a scale μ_0 of the order of the heavy-quark mass m are perturbatively calculable. In the modified minimal subtraction scheme ($\overline{\text{MS}}$) they are given by

$$D_h(x, \mu_0) = \delta(1-x) + \frac{\alpha_s(\mu_0)C_F}{2\pi} \left[\frac{1+x^2}{1-x} \left(\log \frac{\mu_0^2}{m^2} - 2 \log(1-x) - 1 \right) \right]_+ \quad (2.1)$$

$$D_g(x, \mu_0) = \frac{\alpha_s(\mu_0)T_F}{2\pi} (x^2 + (1-x)^2) \log \frac{\mu_0^2}{m^2} \quad (2.2)$$

$$D_i(x, \mu_0) = 0, \quad \text{for } i \neq g, h, \quad (2.3)$$

h being the heavy quark and g the gluon. As usual, $C_F = 4/3$ and $T_F = 1/2$. The notation $[f(x)]_+$ denotes the so-called +-distribution, whose integral against any smooth function $g(x)$ is defined by the equation

$$\int_0^1 g(x) [f(x)]_+ dx = \int_0^1 (g(x) - g(1)) f(x) dx. \quad (2.4)$$

The perturbative fragmentation functions (PFF), evolved up to any scale $\mu \sim p_T$ via the Altarelli–Parisi equations, can be used to evaluate heavy-quark cross sections in the large-transverse-momentum region by convoluting them with short-distance cross sections for massless partons [9, 10, 11], subtracted in the $\overline{\text{MS}}$ scheme. The heavy quark is also treated as a massless active flavour, and therefore also appears in the parton distribution functions of the colliding hadrons and in the evolution of the strong coupling constant³. The differential cross section for the hadroproduction process

$$H_1(P_1) + H_2(P_2) \rightarrow h(P) + X ,$$

following the notations of [9], is given by

$$\begin{aligned} \frac{d^2\sigma}{dp_T^2 dy} = & \frac{1}{S} \sum_{ijk} \int_{1-V+VW}^1 \frac{dz}{z^2} \int_{VW/z}^{1-(1-V)/z} \frac{dv}{1-v} \int_{VW/zv}^1 \frac{dw}{w} \times \\ & \times F_{H_1}^i(x_1, \mu_F) F_{H_2}^j(x_2, \mu_F) D_k(z, \mu_F) \times \\ & \times \left[\frac{1}{v} \left(\frac{d\sigma^0(s, v)}{dv} \right)_{ij \rightarrow k} \delta(1-w) + \frac{\alpha_s^3(\mu_R)}{2\pi} K_{ij \rightarrow k}(s, v, w; \mu_R, \mu_F) \right] , \end{aligned} \quad (2.5)$$

having defined the hadron-level quantities

$$V = 1 + \frac{T}{S}, \quad W = \frac{-U}{S+T}, \quad (2.6)$$

with $S = (P_1 + P_2)^2$, $T = (P_1 - P)^2$ and $U = (P_2 - P)^2$. We also define

$$p_1 = x_1 P_1, \quad p_2 = x_2 P_2, \quad p = P/z \quad (2.7)$$

and

$$s = (p_1 + p_2)^2, \quad t = (p_1 - p)^2, \quad u = (p_2 - p)^2, \quad v = 1 + \frac{t}{s}, \quad w = \frac{-u}{s+t}. \quad (2.8)$$

In terms of the momentum fractions x_1 , x_2 and z , it holds

$$s = x_1 x_2 S, \quad x_1 = \frac{VW}{zv w}, \quad x_2 = \frac{1-V}{z(1-v)}. \quad (2.9)$$

The $\sigma^0(s, v)$ terms represent the leading-order massless-parton to massless-parton scattering cross sections, while the $K_{ij \rightarrow k}(s, v, w; \mu_R, \mu_F)$ represent the NLO corrections, explicitly given in ref. [9].

³For this reason, this resummation formalism is sometimes referred to (somewhat improperly) as the “massless scheme”.

The implementation of the resummation procedure has been performed in ref. [5] for $p\bar{p}$, in [12] for γp , and finally in [13] for $\gamma\gamma$ collisions. In all cases the results agree with the full massive ones (refs. [2], [14] and [15], respectively) in a p_T region from two to four times the mass of the heavy quark. They have a smaller scale dependence than the fixed-order calculations at larger p_T , because the large logarithms originating from gluon emission and gluon splitting are resummed by the evolution of the PFF. In this region they are therefore more reliable (see ref. [5] for a more complete discussion on this point). Because of the intrinsically massless nature of the resummation procedure, these results cannot be trusted when p_T approaches m .

3 The change of scheme

When performing the full FO massive calculation one can, according to ref. [16], conveniently define two renormalization schemes that describe the same physics. One is the usual $\overline{\text{MS}}$ scheme, in which all flavours are treated on an equal footing. The other one, which we will call the decoupling scheme, is similar to the $\overline{\text{MS}}$ scheme except for its treatment of the divergences arising from heavy-flavour loops, which are subtracted at zero external momenta. In the decoupling scheme, for processes taking place at energies much below the heavy-quark mass, we can forget about the heavy flavour altogether. Thus, in QCD, one can define a standard $\overline{\text{MS}}$ scheme, as well as decoupling schemes in which the top, or the top and the bottom, or the top, the bottom and the charm are treated as heavy. It is common to refer to the coupling constant in the corresponding schemes as the 6-, 5-, 4- and 3-flavours coupling constant.

We will now focus, for simplicity, on the case in which we have $n_{\text{lf}} = n_f - 1$ massless flavours and a heavy one of mass m . The strong coupling constant in the decoupling scheme and in the standard $\overline{\text{MS}}$ scheme will be referred to as the n_{lf} and n_f flavours couplings respectively. It turns out that the n_{lf} and n_f flavours couplings are identical at a renormalization scale equal to the mass of the heavy quark: [16]

$$\alpha_s^{(n_f)}(\mu_R) = \alpha_s^{(n_{\text{lf}})}(\mu_R) + \mathcal{O}(\alpha_s^3) \quad \text{for } \mu_R = m. \quad (3.1)$$

Thus, using the renormalization group equation we find

$$\alpha_s^{(n_{\text{lf}})}(\mu_R) = \alpha_s^{(n_{\text{lf}})}(m) - b_0^{(n_{\text{lf}})} \alpha_s^2 \log \frac{\mu_R^2}{m^2} \quad (3.2)$$

$$\alpha_s^{(n_f)}(\mu_R) = \alpha_s^{(n_f)}(m) - b_0^{(n_f)} \alpha_s^2 \log \frac{\mu_R^2}{m^2} \quad (3.3)$$

where

$$b_0^{(n)} = \frac{11C_A - 4nT_f}{12\pi}. \quad (3.4)$$

Observe that in the highest-order terms in eqs. (3.2) and (3.3) we do specify neither the n_f (or n_{lf}) label nor the scale in α_s , since the corresponding differences are of higher order. Taking the difference of eqs. (3.3) and (3.2) and using eq. (3.1) we arrive at

$$\alpha_s^{(n_{lf})}(\mu_R) = \alpha_s^{(n_f)}(\mu_R) - \frac{1}{3\pi} T_f \log \frac{\mu_R^2}{m^2} \alpha_s^2 + \mathcal{O}(\alpha_s^3). \quad (3.5)$$

Similarly structure functions for n_{lf} and n_f massless flavours must match when $\mu_F = m$ [17]. More specifically, they must satisfy the conditions

$$\begin{aligned} F_j^{(n_f)}(x, m^2) &= F_j^{(n_{lf})}(x, m^2) \quad \text{for } j \neq h \\ F_h^{(n_f)}(x, m^2) &= 0 \\ F_{\bar{h}}^{(n_f)}(x, m^2) &= 0, \end{aligned} \quad (3.6)$$

where h stands for the heavy flavour. It should be emphasized that this is a property of the $\overline{\text{MS}}$ subtraction scheme, and it is no longer true in other schemes. Using the Altarelli–Parisi evolution equations together with the matching conditions given in eqs. (3.6), one can easily find the appropriate relations between the parton densities with n_{lf} and n_f active flavours for μ of the order of m .

We begin with the Altarelli–Parisi equations for the parton densities with $n_f = n_{lf} + 1$ flavours

$$\frac{\partial F_i^{(n_f)}(x, \mu)}{\partial \log \mu^2} = \frac{\alpha_s^{(n_f)}(\mu)}{2\pi} \sum_j \int_x^1 F_j^{(n_f)}(x/z, \mu) P_{ij}^{(n_f)}(z) \frac{dz}{z}. \quad (3.7)$$

For μ of the order of m , neglecting terms of order α_s^2 , we get

$$F_i^{(n_f)}(x, \mu) - F_i^{(n_f)}(x, m) = \frac{\alpha_s^{(n_f)}(m) \log \frac{\mu^2}{m^2}}{2\pi} \sum_j \int_x^1 F_j^{(n_f)}(x/z, m) P_{ij}^{(n_f)}(z) \frac{dz}{z}. \quad (3.8)$$

Observe that the heavy-quark density at $\mu = m$ vanishes because of eqs. (3.6). We can then exclude it, putting $j \neq h, \bar{h}$ in the sum. For $i = h$ (or $i = \bar{h}$), eqs. (3.6) and

(3.8) yield

$$F_h^{(n_f)}(x, \mu) = \frac{\alpha_s^{(n_f)}(m) \log \frac{\mu^2}{m^2}}{2\pi} \sum_{j \neq h, \bar{h}} \int_x^1 F_j^{(n_f)}(x/z, m) P_{hj}^{(n_f)}(z) \frac{dz}{z}, \quad (3.9)$$

which shows that the heavy-quark density is of order α_s . An equation similar to eq. (3.8) holds for n_{lf} flavours:

$$F_i^{(n_{lf})}(x, \mu) - F_i^{(n_{lf})}(x, m) = \frac{\alpha_s^{(n_{lf})}(m) \log \frac{\mu^2}{m^2}}{2\pi} \sum_{j \neq h, \bar{h}} \int_x^1 F_j^{(n_{lf})}(x/z, m) P_{ij}^{(n_{lf})}(z) \frac{dz}{z}. \quad (3.10)$$

Taking the difference between eqs. (3.8) and (3.10), and using eqs. (3.6) and (3.1) we obtain, for $i \neq h, \bar{h}$:

$$F_i^{(n_f)}(x, \mu) - F_i^{(n_{lf})}(x, m) = \frac{\alpha_s^{(n_{lf})}(m) \log \frac{\mu^2}{m^2}}{2\pi} \sum_{j \neq h, \bar{h}} \int_x^1 F_j^{(n_{lf})}(x/z, m) \left[P_{ij}^{(n_f)}(z) - P_{ij}^{(n_{lf})}(z) \right] \frac{dz}{z}. \quad (3.11)$$

The only splitting function that depends explicitly upon the number of light flavours is the gluon splitting function. We have

$$P_{gg}^{(n_f)}(z) - P_{gg}^{(n_{lf})}(z) = -\frac{2T_F}{3} \delta(1-z), \quad (3.12)$$

which applied to eq. (3.11) gives

$$F_g^{(n_f)}(x, \mu) - F_g^{(n_{lf})}(x, m) = -\frac{T_F \alpha_s^{(n_{lf})}(m) \log \frac{\mu^2}{m^2}}{3\pi} F_g^{(n_{lf})}(x, m). \quad (3.13)$$

The final result is then

$$\begin{aligned} F_{h(\bar{h})}^{(n_f)} &= \mathcal{O}(\alpha_s) \\ F_j^{(n_f)} &= F_j^{(n_{lf})} + \mathcal{O}(\alpha_s^2) \quad \text{for } j \neq h(\bar{h}), j \neq g \\ F_g^{(n_f)} &= F_g^{(n_{lf})} \left[1 - \frac{\alpha_s T_F}{3\pi} \log \frac{\mu^2}{m^2} \right] + \mathcal{O}(\alpha_s^2). \end{aligned} \quad (3.14)$$

These equations are easily understood in the following way. Since at $\mu = m$ the heavy-quark density is zero, it must be only of order α_s if μ is near but not equal to

m . The gluon density is affected at order α_s by the presence of the heavy flavour. For $\mu > m$, there is in fact some more room for the gluons to go into sea heavy flavours, and therefore the gluon density is slightly diminished. Light flavours do not couple directly to the heavy one. They feel its effect only because of the diminished gluon density, since there are less gluons to go into light flavours. But the variation of the gluon density is itself of order α_s , and the probability for a gluon to go into a light fermion is also of order α_s , so that the net effect is of order α_s^2 .

Now we have all we need to translate the heavy-flavour cross section formulae from the decoupling scheme of ref. [16] to the the standard $\overline{\text{MS}}$ scheme. First of all, the effect of the change of scheme on terms of order α_s^3 is of order α_s^4 , and can thus be neglected. On the other hand, the Born term, of order α_s^2 , will give rise to corrections of order α_s^3 . In the case of the $q\bar{q}$ annihilation Born term, the quark densities are unaffected at order α_s , and thus the only correction arises from the coupling constant. We have

$$\sigma_{q\bar{q}}^{(0)} = \frac{[\alpha_s^{(n_f)}(\mu_R)]^2}{m^2} f_{q\bar{q}} = \frac{[\alpha_s^{(n_f)}(\mu_R)]^2}{m^2} f_{q\bar{q}} \left(1 - \alpha_s \frac{2T_F}{3\pi} \log \frac{\mu_R^2}{m^2} \right) + \mathcal{O}(\alpha_s^4). \quad (3.15)$$

In the case of the gg fusion, instead, we obtain symbolically

$$\begin{aligned} [F_g^{(n_f)}(\mu_F)]^2 \sigma_{gg}^{(0)} &= [F_g^{(n_f)}(\mu_F)]^2 \frac{[\alpha_s^{(n_f)}(\mu_R)]^2}{m^2} f_{gg} \\ &= [F_g^{(n_f)}(\mu_F)]^2 \frac{[\alpha_s^{(n_f)}(\mu_R)]^2}{m^2} f_{gg} \left(1 - \alpha_s \frac{2T_F}{3\pi} \log \frac{\mu_R^2}{\mu_F^2} \right). \end{aligned} \quad (3.16)$$

We thus summarize the results of the present section. In order to compute fixed-order heavy-quark cross sections at the $\mathcal{O}(\alpha_s^3)$ level, using the standard $\overline{\text{MS}}$ scheme with n_f flavours for both the coupling and structure functions, the modifications one needs to apply to the partonic cross sections of refs. [1, 2] are the following:

- Add a term $-\alpha_s \frac{2T_F}{3\pi} \log \frac{\mu_R^2}{m^2} \sigma_{q\bar{q}}^{(0)}$ to the $q\bar{q}$ channel cross section.
- Add a term $-\alpha_s \frac{2T_F}{3\pi} \log \frac{\mu_R^2}{\mu_F^2} \sigma_{gg}^{(0)}$ to the gg channel cross section.

Observe that, in case one uses $\mu_F = \mu_R$, there are no corrections to the gluon channel. Furthermore, for any reasonable ranges of scales and masses, these corrections are not large.

In the following, we will always refer to the FO and FOM0 calculations performed in this transformed scheme. We will thus always assume that α_s and the parton densities F_j refer to $\alpha_s^{(n_f)}$ and $F_j^{(n_f)}$.

4 Massless limit of the fixed-order calculation

The massless limit of the fixed-order formulae (in the sense of eq. (1.5)) is obtained via algebraic methods from the results of ref. [2]. As pointed out there, the limiting procedure is non-trivial. In fact, the partonic cross sections at order α_s^3 contain distributions, such as delta functions or principal value singularities. When taking the massless limit, new contributions to these distributions arise. We will not report here the rather boring details of the algebraic procedure we followed. We would like to remark, however, that its correctness can be easily checked in the following way. We compute a heavy-flavour differential cross section at a fixed p_T , rapidity, and centre-of-mass energy. We choose the renormalization and factorization scales equal to p_T . Under these conditions, the mass dependence of the result is confined to the partonic cross sections. In the massless limit approximations, the only remnants of mass dependence are in logarithms of the mass in the $\mathcal{O}(\alpha_s^3)$ terms. Thus, if we plot the FOM0 cross section versus the logarithm of the mass, we get a straight line. On the other hand, if we plot the full FO cross section versus the logarithm of the mass, it should approach the FOM0 result in the limit of small masses. This is in fact what we observe, as can be seen in figs. 1 and 2.

From the figures, it is quite apparent that the massless limit, as well as its implementation for the calculation of hadronic cross sections, was carried out correctly. There are also some important observations to make. The FOM0 cross section is smaller than the massive calculation. On general grounds, one would instead expect the massive calculation to be smaller, because of the reduction of phase space due to the presence of masses. Moreover, at a given p_T , larger amounts of incoming parton momenta are needed if the mass terms are kept, which also reduces the cross section. These arguments are in fact correct: they should be applied to the absolute value of the cross sections rather than to their signed value. The value of the massive cross section does become smaller and smaller as we approach the threshold. It happens, however, that the massless limit cross section, which has constant slope, changes sign at some point, and then keeps growing in absolute value as we approach the threshold.

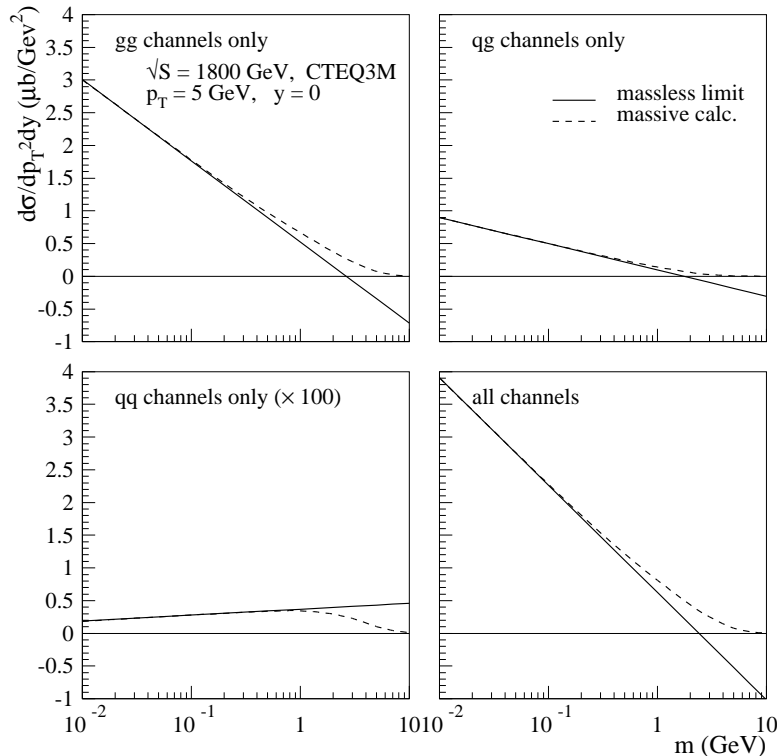


Figure 1: Comparison of the FO and FOM0 differential cross sections as a function of the logarithm of the mass, at $p_T = 5$ GeV.

Notice that the FOM0 approximation is quite inaccurate even at relatively small values of m/p_T . For example, from both figs. 1 and 2 we notice that already at $m/p_T \approx 1/3$, the FO cross section is twice as large as the FOM0 result. In ref. [5] it was observed that for bottom production at the Tevatron, at $p_T \gtrsim 10\text{--}15$ GeV, the resummed cross section agrees quite well with the FO one (although no particular reliability was expected for the resummed approach in that region). Following the results displayed in this section, we must conclude that such an agreement was accidental.

As a concluding remark for this section, we wish to point out that, in principle, the FOM0 result could also be obtained by numerical methods. It would suffice, for any given p_T , to evaluate the FO cross section for a fictitious mass much smaller than p_T and then extrapolate linearly in the logarithm of the mass until the real m , as can be seen from the aforementioned plots. Needless to say, such a method would however be extremely cumbersome, slower and less accurate than the analytical one

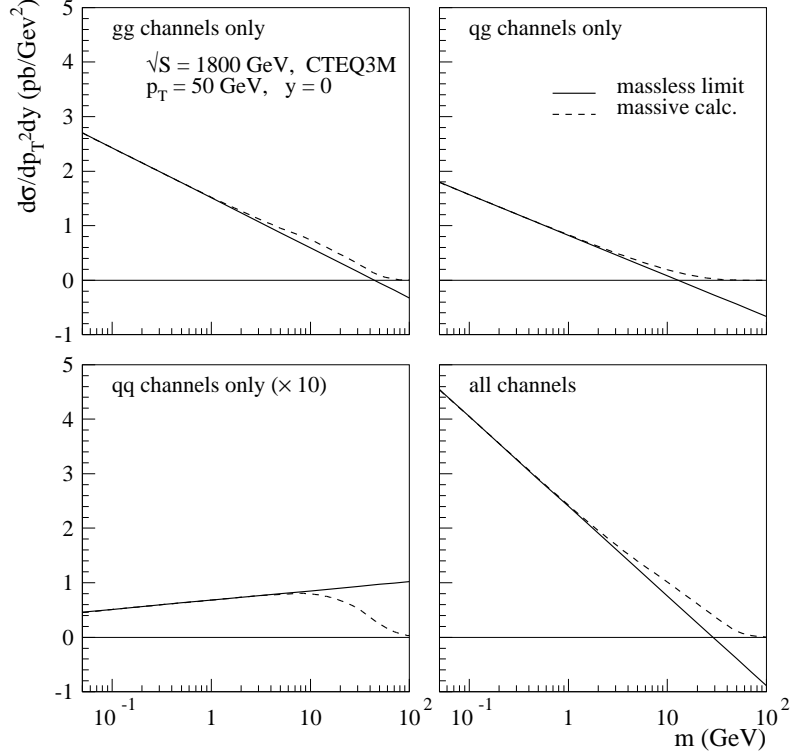


Figure 2: Comparison of the FO and FOM0 differential cross sections as a function of the logarithm of the mass, at $p_T = 50$ GeV.

we have followed.

5 Matching

We now examine the matching between the resummed approach and the FOM0 calculation.

There are ingredients in the resummed approach that are not explicitly present in the FOM0 calculation. These are the fragmentation functions for final-state partons to go into the heavy quark, and the parton density for finding a heavy quark inside the hadron. We take for simplicity $\mu_R = \mu_F = |p_T|$, and denote the common value with μ . The fragmentation function for any parton to go into a heavy quark has a power expansion in terms of the coupling constant evaluated at the scale μ , and of

logarithms of μ/m :

$$D_j(x, \mu, m) = \sum_{k=0}^{\infty} \sum_{l=0}^k d_j^{(k,l)}(x, \mu, m) \log^l \frac{\mu}{m} \alpha_s^k(\mu), \quad (5.1)$$

that can be obtained by solving the evolution equation for the fragmentation function at the NLL level, with the initial conditions (2.1)–(2.3). Similarly, the parton density for finding the heavy flavour in the hadron can be expanded in the form

$$F_h(x, \mu, m) = \sum_{k=0}^{\infty} \sum_{l=0}^k f^{(k,l)}(x, F_l(\mu)) \log^l \frac{\mu}{m} \alpha_s^k(\mu). \quad (5.2)$$

With $F_l(\mu)$ in the argument of the coefficients, we mean that the coefficients have a complicated *functional* dependence upon the parton densities evaluated at the scale μ . The existence of formal expansions of the form (5.1) and (5.2) can be easily proved, by writing the Altarelli–Parisi equations in integral form, and then solving them iteratively. We present a more detailed argument in Appendix A.

Once eqs. (5.1) and (5.2) are formally substituted in the RS cross section formula, this formula itself becomes a power expansion of the form of eq. (1.2), with the coefficients that depend (functionally) upon the structure functions for light partons, in the n_f -flavours scheme, evaluated at the scale μ . The FOM0 calculation has an expansion of the same form (truncated to order α_s^3) with coefficients that are also dependent upon the same light-parton structure functions⁴ evaluated at the scale μ . Thus, because of the next-to-leading logarithmic accuracy of the resummed cross section, the terms up to the order α_s^3 will match exactly with the FOM0 calculation.

This property of the resummed calculation is built into the resummation formalism of ref. [5]. In this work, we have explicitly verified this matching by comparing the numerical value of the FOM0 and RS approaches in the limit $\alpha_s \rightarrow 0$.

In order to do this, we need to vary the coupling constant towards very small values, in order to check if the difference of the two approaches is indeed of order α_s^4 . We thus need an explicit expression for the fragmentation functions and for the heavy-flavour parton density in terms of $\alpha_s(\mu)$. For our purpose, it is, however, sufficient to have an approximation for these quantities that is valid at order α_s . These are easily

⁴We observe that this property of the FOM0 calculation is only valid in the modified scheme described in section 3. If we had used the standard scheme for the fixed-order calculation, the structure functions and the coupling α_s appearing there would be those with $n_f - 1$ flavours.

obtained. For the heavy-flavour parton density we use

$$F_h(x, \mu) = \frac{\alpha_s(\mu) \log \mu^2/m^2}{2\pi} \int_x^1 F_g(x/z, \mu) P_{hg}(z) \frac{dz}{z}, \quad (5.3)$$

which equals the corresponding expression in eq. (3.9) up to terms of higher order in α_s . For the $\overline{\text{MS}}$ fragmentation functions we instead simply use the initial conditions eqs. (2.1,2.2) evaluated at the large scale $\mu = p_T$ and without evolution. This is the first term in the expansion of eq. (5.1). We thus perform the RS computation with these approximate parton densities and fragmentation functions; we call this approximation RSA. In comparing RSA and FOM0 we vary α_s from its true value at the given p_T to $1/3$, $1/10$ and $1/30$ of it. The results are collected in fig. 3. The interpretation of the figure is quite obvious. The $\mathcal{O}(\alpha_s^2)$ result in the FOM0

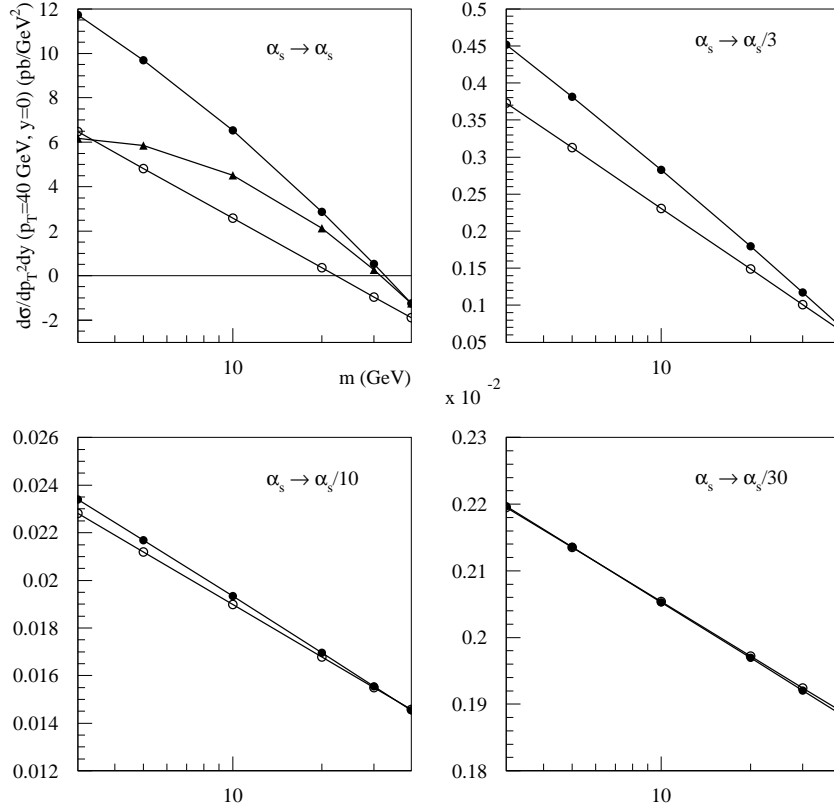


Figure 3: Matching of the FOM0 and RS computations for small α_s , for $p_T = 40$ GeV and $y = 0$. The colliding hadrons are $p\bar{p}$ at $\sqrt{S} = 1.8$ TeV. The triangles represent the RS computation, the full circles the RSA, and the empty circles the FOM0.

calculation does not depend upon the mass of the heavy quark, since it does not

contain any logarithm. The slope of the FOM0 result is only due to $\mathcal{O}(\alpha_s^3)$ terms, as in figs. 1 and 2. In fact, we see that the relative slope of the result decreases roughly like α_s , and the relative difference between the RSA and the FOM0 result also decreases as α_s^2 . This demonstrates that the difference between the RSA and FOM0 results is of order α_s^4 , as expected.

In the upper-left plot of fig. 3, the full RS result (triangles) is also shown, evaluated with $\mu_F = \mu_R = p_T$. We see that, if the mass is not too small, the full RS result agrees reasonably well with the approximate RSA one, the two being of course coincident when $m = p_T$, and therefore no evolution whatsoever is taking place.

We observe that, at physical values of α_s , and for masses of the order of the transverse momentum, the RS cross section differs significantly from the FOM0 one, in spite of the fact that their difference is formally of order α_s^4 . This is unfortunate, since it is precisely in this region ($p_T \sim m$) that we would like to see a smooth matching between the FO result and the FONLL one, and this can only happen if the FOM0 and the RS calculations cancel to a high extent.

6 Power effects in the RS and FOM0 calculations

When comparing and matching the FO, FOM0 and RS approaches, there is a lot of arbitrariness in the way mass effects are treated. For example, we may decide to compare transverse-mass distributions instead of transverse momenta. These are equal for the FOM0 and RS calculations, but differ in the FO case. The difference is shown in the two plots of fig. 4, where the cross section is plotted as a function of the mass, keeping either m_T or p_T fixed. If we focus upon the Born result, it is quite easy to understand the differences in the two plots. The massive result is closer to the massless one when the transverse mass is kept fixed, i.e. in the left plot. In fact, in this case, the differences come only from mass effects in the matrix elements, and these effects are not large. On the other hand, if the transverse momentum is kept fixed (right plot), as the mass grows the FO Born result requires more incoming momenta from the structure functions, and this suppresses the cross section. This mechanism is also at work, of course, in the NLO result. However, in this case, the FOM0 approximation is bound to fail more radically, because of its linear dependence in $\log p_T/m$: for large masses, it changes sign, which is clearly unphysical. Of course, it could be argued that the correct form of the logarithm in the massless approximation

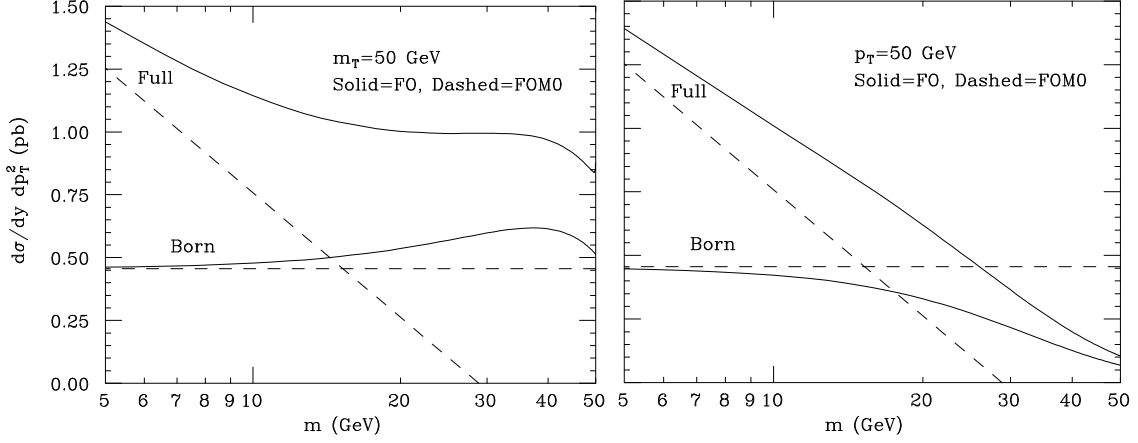


Figure 4: FO versus FOM0 at Born and full $\mathcal{O}(\alpha_s^3)$ level, plotted as a function of the mass and at fixed transverse mass (left figure) or fixed transverse momenta (right figure).

should be something like $\log(p_T^2 + m^2)/m^2$, but the point is that the only use of the FOM0 computation is to subtract it from the available RS result, which only contains logarithms of p_T/m .

We will therefore proceed as follows. For a given transverse momentum p_T , the FO cross section is evaluated and combined, using eq. (1.6), with the FOM0 and RS results evaluated instead at the corresponding $m_T = \sqrt{p_T^2 + m^2}$ value. In this way the three calculations are performed at the same m_T . Moreover, a central choice for the renormalization and factorization scales will be $\mu_R = \mu_F = \sqrt{p_T^2 + m^2}$, so that they coincide in the three calculations.

Having done so, one has further freedom in the choice of the function $G(m, p_T)$, the factor multiplying the RS – FOM0 term in eq. (1.6). $G(m, p_T)$ should approach 1 at large p_T . It could in fact be chosen equal to 1. However, as we showed in sect. 5, the difference RS – FOM0, although of order α_s^4 , is abnormally large. We interpret this as a consequence of the fact that, when p_T is near m , the massless approximation becomes completely meaningless. This is also visible from the left plot of fig. 4, where we can see that the FOM0 result starts to deviate significantly from the full FO one when the mass becomes larger than about one fifth of m_T . For a physical b quark, with a mass of 5 GeV, this means that we should suppress the RS – FOM0 term for p_T smaller than about 20–25 GeV. This seemingly large value is in fact not so difficult to justify. The dominant logarithmic effects come in fact from the flavour-excitation

and gluon-splitting graphs. In order for a gluon-splitting phenomenon to be a truly collinear process, and thus dominant over power-suppressed terms, the incoming gluon must carry a transverse mass that should be more than four times the mass of the heavy quark, in such a way that the produced heavy quark and antiquark are both relativistic. Most of this momentum should end up in the quark (the cases in which the momentum is evenly shared is suppressed by the luminosity). A similar reasoning also applies to the flavour excitation case.

We thus choose $G(m, p_T) = p_T^2/(p_T^2 + c^2 m^2)$, and our final formula becomes

$$\text{FONLL} = \text{FO} + \frac{p_T^2}{p_T^2 + c^2 m^2} [\text{RS} - \text{FOM0}] , \quad (6.1)$$

with $c = 5$, which suppresses the resummation correction $\text{RS} - \text{FOM0}$ for $m_T < 5m$.

Before closing this section it is important to recall how all these manipulations involving power-suppressed mass terms only affect terms of order α_s^4 or higher. Whatever theoretical uncertainty might stem from them, we must live with it, as these terms have never been computed.

7 An LL implementation of the matching procedure

We will now focus on a first implementation of our formalism, in which only leading logarithms are resummed. Our resummed formula will have the following form

$$\text{FOLL} = \text{FO} - \text{FOM0LL} + \text{RSL} , \quad (7.1)$$

where for simplicity we have chosen $G(m, p_T) = 1$. The meaning of the various terms is as follows: FOLL is our fixed-order plus leading-log result, FOM0LL is the leading logarithmic part of FOM0, and RSL is the leading logarithmic part of the RS result. Thus FOM0LL contains terms proportional to α_s^2 and $\alpha_s^3 \log \mu/m$, but no terms proportional to α_s^3 alone. More specifically, in the notation of eq. (1.5) we have

$$\text{FOM0LL} = a_0 \alpha_s^2 + a_1 \log \frac{\mu}{m} \alpha_s^3 . \quad (7.2)$$

The FOM0LL contribution precisely cancel the terms up to order α_s^3 in RSL. Thus, the difference $\text{RSL} - \text{FOM0LL}$ begins with terms of order $\alpha_s^4 \log^2 \mu/m$. Therefore, we have an interpolating formula that reduces to the NLO result for small p_T , and sums all the leading logarithms in the large- p_T limit. Our FOLL results are illustrated in

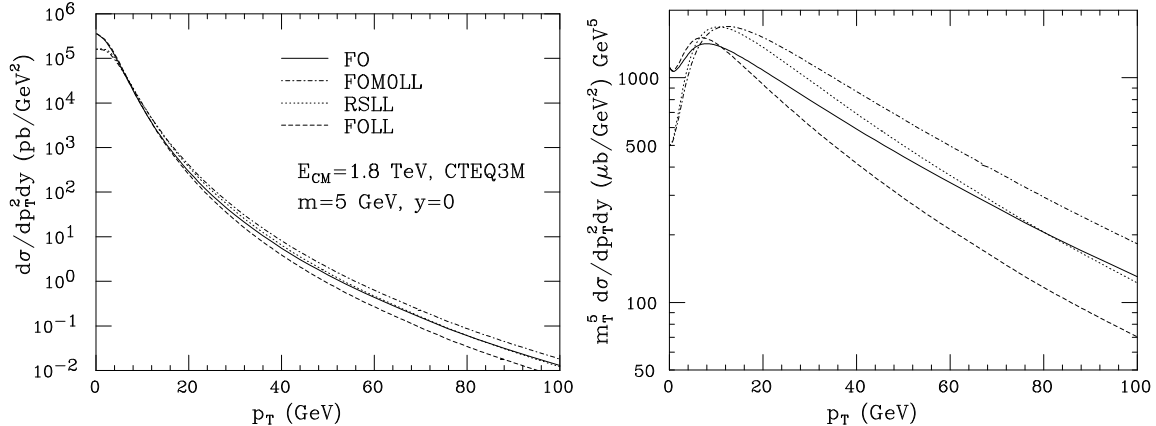


Figure 5: Illustration of the FOLL result for the central values of the scales

$$\mu_F = \mu_R = m_T.$$

figs. 5 and 6. From fig. 5, which is obtained with a choice of scales $\mu_R = \mu_F = m_T$, we see that the FOM0LL and the RSL curves coincide at $p_T = 0$, corresponding to $\mu = m_T = m$. This is because their difference is made up of terms of the form $\alpha_s^2(\alpha_s \log \mu/m)^k$ for $k \geq 2$, and thus vanishes for $\mu = m$. They also depart relatively slowly from each other, since there are at least two powers of logarithms in their difference. As a consequence of this fact, the difference between the FO and the FOLL curves vanishes at small p_T . The FOLL curve undershoots instead the FO curve at larger p_T , in agreement with what was estimated in ref. [2].

There is a basic difference between the FOLL approach and the FONLL one. In the latter approach, it was mandatory to keep the same scales μ_R and μ_F in all terms of the defining equation (1.6). In eq. (7.1), on the other hand, while it is important to maintain the same scale in the last two terms (in order for their difference to be of order α_s^4), this scale could differ from the one used in the FO term. In fact, the difference $\text{RSL} - \text{FOM0LL}$ is a sum of terms proportional to $\alpha_s^2(\alpha_s \log \mu/m)^k$, and their scale variation is thus of next-to-leading order (i.e. it contains an extra power of α_s or one less power of $\log \mu/m$). Thus, by a change of scale in the $\text{RSL} - \text{FOM0LL}$ difference with respect to the FO scale, one obtains an equivalent formula, up to the addition of next-to-leading logarithmic terms, which are not fully specified in this approximation.

This observation leads to the conclusion that no improvement in the scale dependence can be observed if only LL resummation is performed, or better, if an

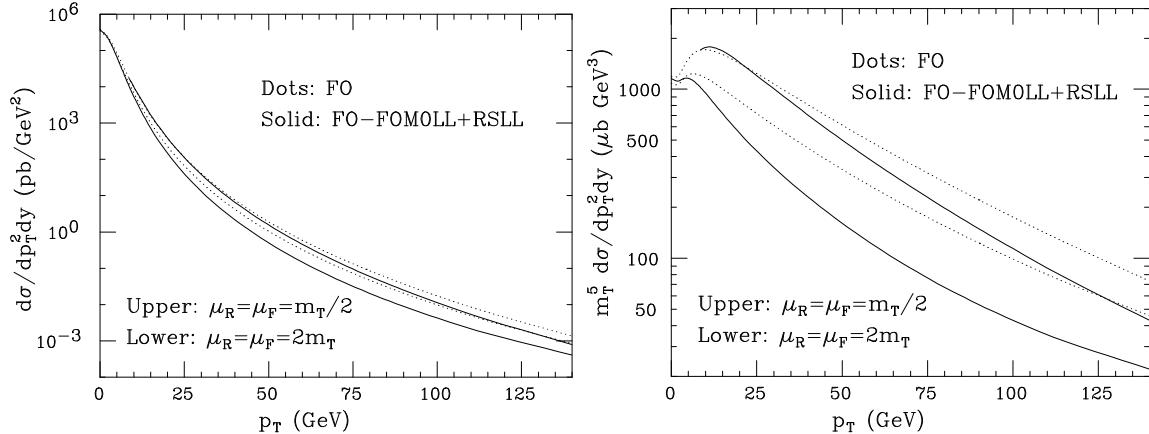


Figure 6: Illustration of the FOLL result for two scale choices.

improvement is observed it must be accidental. The reader may now wonder where the improvement lies in this case of LL resummation, since undoubtedly we did resum a tower of dominant terms. One can easily convince oneself that the improvement lies in the fact that, for a choice of scales near p_T , the large logarithms in eq. (7.1) are resummed, and thus one is justified to consider only scale variations for scales of the order of p_T . This point may sound confusing, since for heavy-flavour cross sections at high transverse momenta the error is usually estimated by varying the scale in a neighbourhood of p_T . We remind the reader that this procedure is not obvious at all: since we are facing a two-scale problem, one should vary the scale between m and p_T . The justification for using the upper range $\mu \approx p_T$ only was outlined in ref. [2]. In that paper the scale was varied in the neighbourhood of p_T , but subleading logarithms were estimated, and included in the error. Since they turned out to be small, they were no longer included in subsequent works.

Having said that, we do not expect a scale improvement in the FOLL formula. The scale dependence of our FOLL result, displayed in fig. 6, is indeed not smaller than the scale dependence of the FO result.

It is now time to comment on the results of ref. [6]. There, the NLO fixed-order result is fully included in the calculation, but the resummation is only performed with leading-logarithmic level accuracy. The authors do find a reduction in the scale dependence at moderate p_T , while at large p_T they find stronger scale dependence. From the considerations given in the present section, we conclude that, in fact, the scale compensation they observe can only be accidental.

8 Alternative choice of fragmentation scheme

As pointed out in sect. 7, the RS and FOM0 results do not agree at the point $m = p_T$ (for the choice of scale $\mu = p_T$), where we would like to see, instead, a cancellation. Furthermore, also the slopes of the two curves are quite different at this point. These two differences can easily be traced back to two kinds of terms that arise in the RS calculation when convoluting the NLO, $\overline{\text{MS}}$ subtracted massless kernels with the structure and fragmentation functions. The offset of RS with respect to FOM0 is due to spurious α_s^4 terms, originating from the product of $\mathcal{O}(\alpha_s^3)$ terms in the kernel cross sections with the non-logarithmic $\mathcal{O}(\alpha_s)$ term in the D_h fragmentation function initial condition of eq. (2.1). These terms do not contain logarithms of p_T/m , and thus remain different from zero at $p_T = m$. They are not correctly predicted by the RS calculation, which is accurate up to terms proportional to $\alpha_s^4 \log(p_T/m)$. The difference in slope is, instead, due precisely to terms of this kind. They are correctly given by the RS formalism, but not included in the FOM0 result.

While nothing can be done to solve this second problem, it is instead possible to try to eliminate the first one. This can be done by switching from the standard $\overline{\text{MS}}$ scheme to a new factorization scheme where the initial condition for the heavy-quark to heavy-quark fragmentation function, eq. (2.1), does not contain the non-logarithmic $\mathcal{O}(\alpha_s)$ term and is therefore a delta-function for $\mu_0 = m$. We call this scheme the *Delta scheme* (DL). The transformation to go from the $\overline{\text{MS}}$ scheme to the DL scheme is described in detail in Appendix B. The effect of the scheme change can be appreciated in fig. 7, where the cross section is again plotted as a function of the logarithm of the mass. One can clearly see how the DL result agrees with the FOM0 one at the point $m = p_T$, thereby providing the desired cancellation. However, the slope remains different.

For comparison, we also plot the RSLL result. This does not contain the $\alpha_s^4 \log(p_T/m)$ terms, and has therefore the same slope as the FOM0 result. Its offset with respect to the FOM0 result is instead due to the non-logarithmic α_s^3 term, which is present there.

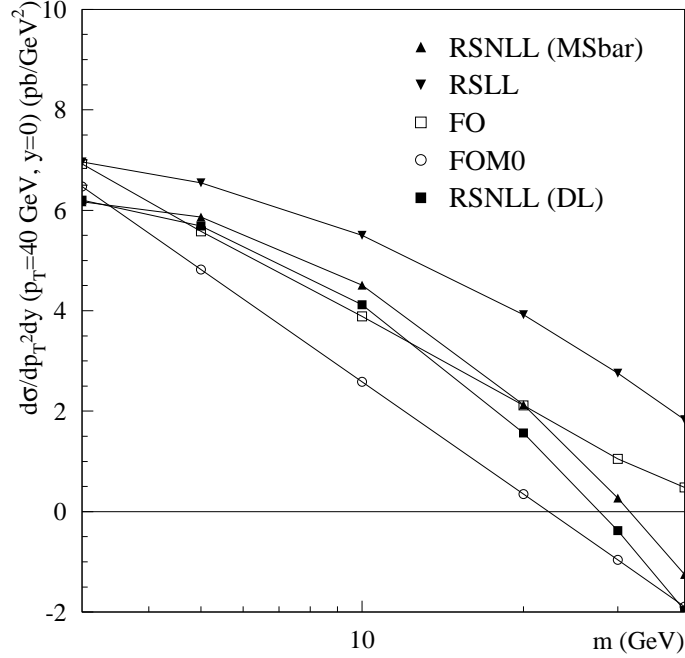


Figure 7: Dependence of the cross section on the logarithm of the mass, at $p_T = 40$ GeV. Shown are the full FO result (empty squares), the FOM0 massless limit (empty circles), the LL resummed result (downward-facing triangles), the RS result both in the $\overline{\text{MS}}$ (upward-facing triangles) and in the DL (full squares) schemes.

9 Some numerical NLL results

This section collects the final NLL results for the heavy quark cross section, as obtained from combining the fixed-order massive result with the resummed one.

We begin by combining the various terms with the choice of scales $\mu_R = \mu_F = \mu = m_T$. For the sake of discussion, we now use $G(m, p_T) = 1$, corresponding to the choice $c = 0$ in eq. (6.1). Figure 8 shows the full massive result (FO) compared with the combined ones, both in the $\overline{\text{MS}}$ and in the DL schemes.

We can first of all appreciate the effect of switching from the $\overline{\text{MS}}$ to the DL scheme. In the latter the FONLL result coincides with the FO one at the $p_T = 0$ (and hence $\mu = m_T = m$) point, as desired, while the result in the $\overline{\text{MS}}$ scheme presents an offset. This is directly related to the offset previously noticed in fig. 7, at the $m = p_T$ point. It is worth mentioning how the cancellation in the DL scheme still relies on our choice of factorization scale $\mu_F = \sqrt{m^2 + p_T^2}$, which ensures $\mu_F = m$ at $p_T = 0$. Any

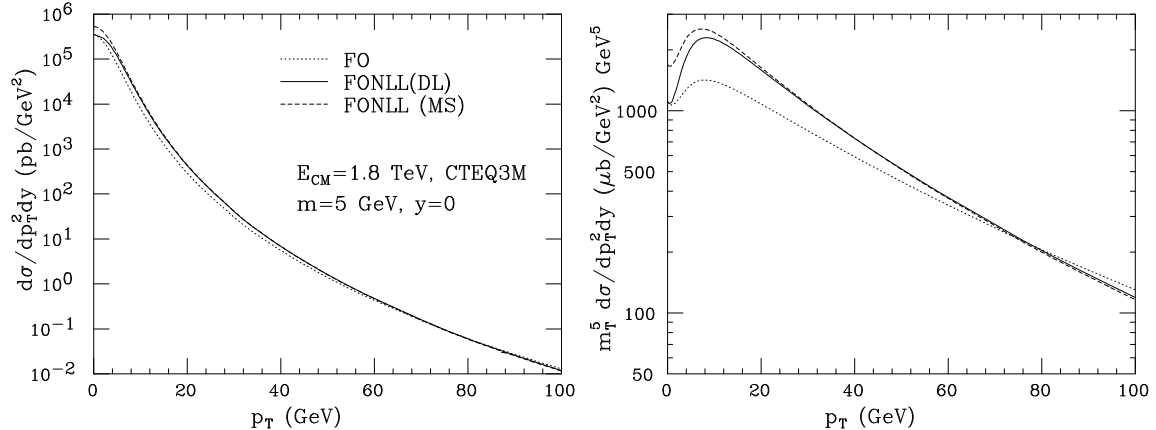


Figure 8: Combined cross section, both in the $\overline{\text{MS}}$ and in the DL schemes, obtained with $c = 0$.

other scale choice will destroy the matching at this point, giving results qualitatively similar to those obtained in the $\overline{\text{MS}}$ scheme. This will appear evident when we will present the bands obtained by varying the renormalization/factorization scales.

We now describe the procedure we follow in order to obtain our final theoretical result, including the errors estimated by varying the factorization and renormalization scale. First of all, we fix $c = 5$, as discussed in sect. 6. Our prediction band is the envelope of the curves obtained by varying the renormalization and factorization scales in the range $[m_T/2, 2m_T]$. We also distinguish in our calculation the factorization scale for the structure functions from the one for the fragmentation functions, varying them independently. The resulting bands, for both the $\overline{\text{MS}}$ and the DL schemes, are shown in figs. 9 and 10.

A few interesting observations can be made about these plots. First of all, the band of the combined result is much narrower in the large- p_T region. This result had already been found with the resummed calculation of ref. [5], and is the expected outcome of the resummation of the large $\log(p_T/m)$ terms. Further, we notice that the combined bands match exactly the FO ones at $p_T \rightarrow 0$. This feature is due to the suppression factor $G(m, p_T)$, which annihilates completely the RS – FOM0 term at this point. Without this suppression the band would be very large in this region, owing to the uncontrolled behaviour of the massless approximation at small p_T . Last, the combined band lies in the intermediate- p_T region, a little above the FO one, and is about equally wide. The maximum increase is of the order of 10%–20% on the

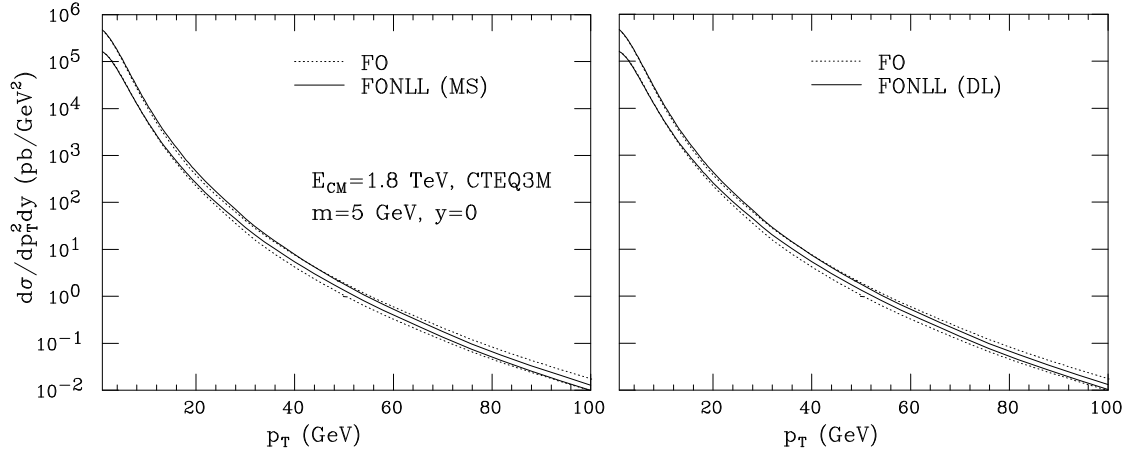


Figure 9: Combined cross section, both in the $\overline{\text{MS}}$ and in the DL schemes. Shown are the bands obtained by varying independently the renormalization and factorization scales. A suppression factor of the small p_T region, according to eq. (6.1), with $c = 5$, is included.

NLO full massive result. We also notice that the DL and $\overline{\text{MS}}$ schemes give about the same result: no significant differences can be observed.

The Tevatron results for b production are usually given in terms of a cross section with a cut $p_T > p_T^{\text{min}}$. In order to give a rough estimate of the effect of resummation for this quantity, relative to the NLO calculation, we plot it in fig. 11. Since this is only included as an indication, and since the cross section is reasonably uniform in rapidity in the central region, we do not perform the y integration in the range $|y| < 0.5$.

In summary, we observe that our resummation procedure indicates the presence of a small enhancement in the intermediate p_T region, followed by a reduction of the cross section (and of the uncertainty band) at larger p_T . The question we should now ask is how reliable this enhancement is. Of course, if we used smaller values for the parameter c , the cross section at moderate p_T would increase, thus helping in explaining the discrepancy between theory and the Tevatron data. However, the considerations given in sect. 6 do indicate that $c = 5$ is the conservative choice we should make to obtain a reliable result.

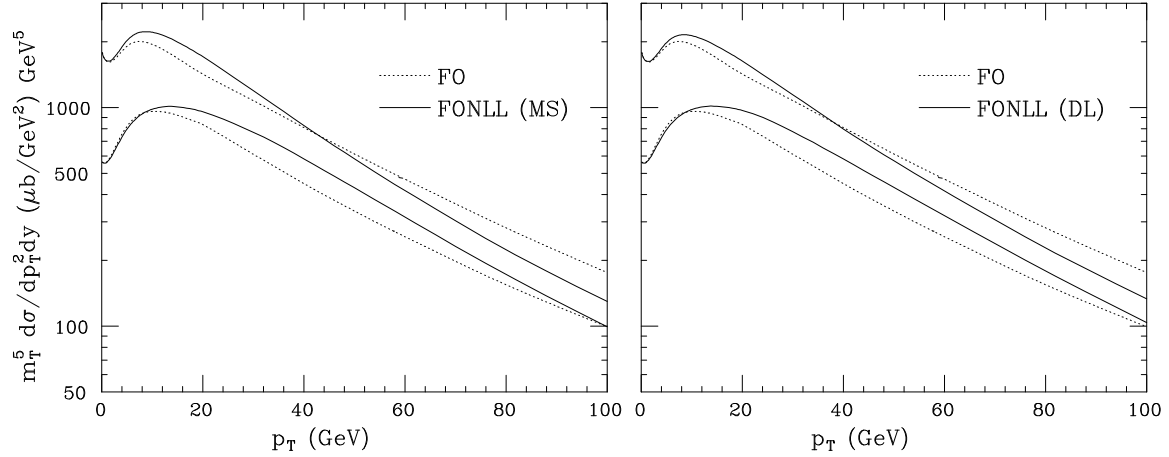


Figure 10: Same as in fig. 9, with an m_T^5 weight.

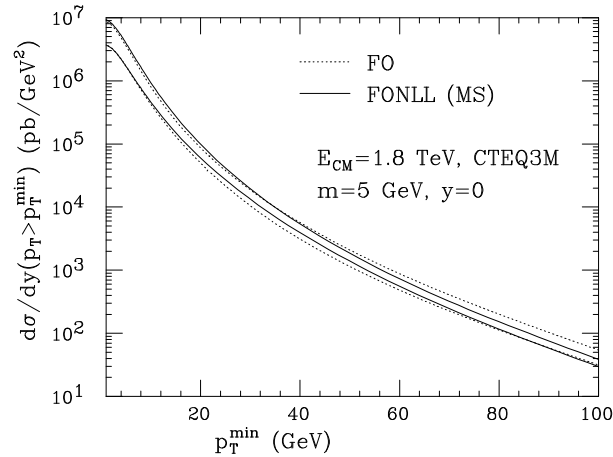


Figure 11: The b cross section per unit rapidity as a function of the p_T cut.

10 Conclusions

In summary, we have defined a procedure for improving in a systematic way the calculation of the transverse-momentum heavy-flavour spectrum. Using already available calculations, this procedure has been applied to obtain the p_T spectrum of heavy-flavour production with NLO accuracy in α_s , and with NLL resummation of logarithms of p_T/m .

This calculation confirms essentially the results of refs. [2] and [5], to which it

reduces in the small- and large- p_T limit, respectively. In the intermediate transverse momentum region, when p_T is roughly between two times and five times the heavy quark mass, we find a slight enhancement of the cross section with respect to previous results.

We can understand this enhancement in two ways. In relation to the calculation of ref. [5], we find that mass corrections at order α_s^2 and α_s^3 , not included there, are large and positive in this region. In relation to the calculation of ref. [2], instead, we find large resummation corrections, arising at the next-to-leading order level. For example, large contributions arise from the notoriously large corrections to the parton cross sections for the $gg \rightarrow g + X$ process, convoluted with the gluon fragmentation into heavy quark. These contributions are of order α_s^4 (if one accounts for the fact that the gluon fragmentation into a heavy quark is of order α_s), and therefore are not included in the α_s^3 calculation of ref. [2].

In our calculation, we had the freedom to suppress resummation effects of order higher than α_s^3 in the small-transverse-momentum region. We included such a suppression, based upon the comparison of the full massive- and massless-limit calculations at order α_s^3 . Since we found that the massless limit result is not a good approximation to the massive one for $p_T \lesssim 5m$, our suppression factor begins to act precisely in that region.

In the present work, we have only developed the basic formalism for a reliable computation of the heavy-quark p_T spectrum. The enhancement we found goes in the direction of favouring a better comparison with the Tevatron data on b production. Other ingredients should, however, be included in a full phenomenological analysis. A non-perturbative fragmentation-function contribution, for example, should be extracted from e^+e^- data (see for example [18, 19]) and carefully included in the computation. Similarly, theoretical uncertainties arising from the error in the determination of the strong coupling constant, of the structure functions and of the b -quark mass should be fully assessed in order to give a reliable theoretical prediction. We will address these problems in future work.

Acknowledgements.

One of us (M.C.) would like to thank the Theory Division at CERN for its kind hospitality during the completion of this work.

This work was supported in part by the EU Fourth Framework Programme “Training and Mobility of Researchers”, Network “Quantum Chromodynamics and the Deep

Structure of Elementary Particles”, contract FMRX-CT98-0194 (DG 12 - MIHT).

Appendix A: Perturbative expansion of the heavy-quark parton density

We now prove the existence of expansions of the form of eqs. (5.1) and (5.2). We consider the Mellin transforms of the fragmentation functions and structure functions. We will use the notation

$$D_i(\mu_0) = \int \frac{dx}{x} x^N D_i(x, \mu_0) , \quad (\text{A.1})$$

and a similar one for the structure functions. Thus, every time that the x dependence is not given explicitly we refer to the Mellin transforms of the corresponding quantity.

It is well-known that fragmentation functions at a scale μ are given in terms of the fragmentation functions at a scale μ_0 (in matrix notation) by an equation of the form

$$D(\mu) = (1 + M(\alpha_s(\mu), \log \mu/\mu_0)) D(\mu_0) , \quad (\text{A.2})$$

where 1 stands for the identity matrix, and M is a matrix whose elements are power expansions in $\alpha_s(\mu)$ and $\log \mu/\mu_0$, starting at order $\alpha_s(\mu)$, and having in all their terms no more powers of $\log \mu/\mu_0$ than powers of α_s . We choose $\mu_0 = m$, replace $D(m)$ with its power expansion in terms of $\alpha_s(m)$, which contains no logarithms, and replace $\alpha_s(m)$ with its power expansion in terms of $\alpha_s(\mu)$, which does contain logarithms, but always with a smaller power than the corresponding power of $\alpha_s(\mu)$. With these operations we put $D(\mu)$ in the form of eq. (5.1).

For eq. (5.2), we begin with a similar equation for structure functions

$$F(\mu_0) = (1 + M(\alpha_s(\mu), \log \mu/\mu_0)) F(\mu) , \quad (\text{A.3})$$

choose $\mu_0 = m$, and separate the h and \bar{h} and the light components l

$$\begin{aligned} F_{h/\bar{h}}(m) &= F_{h/\bar{h}}(\mu) + M_{h/\bar{h},j}(\alpha_s(\mu), \log \mu/m) F_j(\mu) , \\ F_l(m) &= F_l(\mu) + M_{l,j}(\alpha_s(\mu), \log \mu/m) F_j(\mu) . \end{aligned} \quad (\text{A.4})$$

Observe that the index j runs also on h and \bar{h} . The left-hand side of the first two equations can be given as a power expansion in $\alpha_s(m)$, with coefficients proportional

to the $F_l(m)$. They in fact start at order α_s^2 in the $\overline{\text{MS}}$ scheme. The $F_l(m)$ can be obtained from the remaining equations. Furthermore, $\alpha_s(m)$ can be expanded in powers of $\alpha_s(\mu)$ as before. The first two equations can then be solved for $F_{h/\bar{h}}(\mu)$ (since the coefficients in front of the $F_{h/\bar{h}}(\mu)$ terms begin with 1, and can therefore be inverted). The expressions for the $F_{h/\bar{h}}(\mu)$ components will be linear functions of the $F_l(\mu)$, with coefficients that are power expansions in $\alpha_s(\mu)$ and in $\log \mu/m$, with no more powers of logarithms than powers of $\alpha_s(\mu)$, as in eq. (5.2).

Appendix B: The DL scheme

We now discuss the change of scheme from the $\overline{\text{MS}}$ to the DL scheme. This will be given, for the fragmentation functions and for the next-to-leading evolution kernels, in terms of Mellin transforms, defined according to eq. (A.1).

Using the notation of [20], we can describe the evolution in terms of the variable

$$t = \frac{2}{b_0} \log \frac{\alpha(\mu_0^2)}{\alpha(\mu)} \quad (\text{B.1})$$

instead of μ . Calling $E(\mu, \mu_0)$ the evolution matrix from μ_0 to μ (in N space), we have

$$\begin{aligned} \frac{dE(\mu, \mu_0)}{dt} &= \left(P_0 + \frac{\alpha(\mu)}{2\pi} R \right) E(\mu, \mu_0) \\ R &= P_1 - \frac{b_1}{2b_0} P_0. \end{aligned} \quad (\text{B.2})$$

The fragmentation functions in the $\overline{\text{MS}}$ scheme are given at the low scale by eqs. (2.1)–(2.3), which we rewrite here as

$$\begin{aligned} D_h(\mu_0) &= 1 + \frac{\alpha(\mu_0)}{2\pi} P_{qq} \log \frac{\mu_0^2}{m^2} + \frac{\alpha(\mu_0)}{2\pi} d_1 + \mathcal{O}(\alpha^2) \\ D_g(\mu_0) &= \frac{\alpha(\mu_0)}{2\pi} P_{gq} \log \frac{\mu_0^2}{m^2} + \mathcal{O}(\alpha^2) \\ D_{i \neq h, g}(\mu_0) &= \mathcal{O}(\alpha^2). \end{aligned} \quad (\text{B.3})$$

where

$$d_1 = - \int \frac{dx}{x} x^N C_F \left[\frac{1+x^2}{1-x} (2 \log(1-x) + 1) \right]_+$$

$$\begin{aligned}
P_{qq} &= \int \frac{dx}{x} x^N C_F \left[\frac{1+x^2}{1-x} \right]_+ \\
P_{qg} &= \int \frac{dx}{x} x^N T_F [(1-x)^2 + x^2] .
\end{aligned} \tag{B.4}$$

We want a scheme \tilde{D} where

$$\tilde{D}_h(\mu_0) = 1 + \frac{\alpha(\mu_0)}{2\pi} P_{qq} \log \frac{\mu_0^2}{m^2} \tag{B.5}$$

and the other components of the fragmentation function remain identical.

The transformations

$$\begin{aligned}
\tilde{D}_h(\mu) &= \left(1 - \frac{\alpha(\mu)}{2\pi} d_1 \right) D_h(\mu) \\
\tilde{D}_i(\mu) &= D_i(\mu) \quad \text{for } i \neq h
\end{aligned} \tag{B.6}$$

have precisely this property, that is to say they translate eqs. (B.3) into

$$\begin{aligned}
\tilde{D}_h(\mu_0) &= 1 + \frac{\alpha(\mu_0)}{2\pi} P_{qq} \log \frac{\mu_0^2}{m^2} + \mathcal{O}(\alpha^2) \\
\tilde{D}_g(\mu_0) &= \frac{\alpha(\mu_0)}{2\pi} P_{gq} \log \frac{\mu_0^2}{m^2} + \mathcal{O}(\alpha^2) \\
\tilde{D}_{i \neq h,g}(\mu_0) &= \mathcal{O}(\alpha^2) .
\end{aligned} \tag{B.7}$$

Having changed the initial conditions, we now need to find the modifications to the evolution equations and to the short-distance cross sections. Defining the matrix

$$C_{ij} = -\delta_{ij} d_1 \quad \text{for } i \neq g, \quad C_{ig} = C_{gi} = 0, \quad C_{gg} = 0, \tag{B.8}$$

we have

$$\tilde{D} = \left(1 + \frac{\alpha_s}{2\pi} C \right) D \tag{B.9}$$

where we imply vector and matrix notation when we omit the indices.

Since physical quantities should remain unchanged, we must have

$$\hat{\sigma}_i(\mu) E_{ij}(\mu, \mu_0) D_j(\mu_0) = \tilde{\sigma}_i(\mu) \tilde{E}_{ij}(\mu, \mu_0) \tilde{D}_j(\mu_0) . \tag{B.10}$$

To satisfy the above equality, we define

$$\begin{aligned}
\tilde{E}(\mu, \mu_0) &= \left(1 + \frac{\alpha(\mu)}{2\pi} C \right) E(\mu, \mu_0) \left(1 - \frac{\alpha(\mu_0)}{2\pi} C \right) \\
\tilde{\sigma}(\mu) &= \hat{\sigma} \left(1 - \frac{\alpha(\mu)}{2\pi} C \right)
\end{aligned} \tag{B.11}$$

We now derive the evolution equation for \tilde{E} . We use the obvious observation that $(1 - \alpha(\mu)/2\pi C)\tilde{E}$ obeys the same evolution equation as E

$$\frac{d}{dt} \left[\left(1 - \frac{\alpha(\mu)}{2\pi} C \right) \tilde{E}(\mu, \mu_0) \right] = \left(P_0 + \frac{\alpha(\mu)}{2\pi} R \right) \left[\left(1 - \frac{\alpha(\mu)}{2\pi} C \right) \tilde{E}(\mu, \mu_0) \right] . \quad (\text{B.12})$$

Since

$$\frac{d\alpha(\mu)}{dt} = -\frac{b_0}{2}\alpha(\mu) \quad (\text{B.13})$$

we get

$$\begin{aligned} \frac{b_0}{2} \frac{\alpha(\mu)}{2\pi} C \tilde{E}(\mu, \mu_0) + \left(1 - \frac{\alpha(\mu)}{2\pi} C \right) \frac{d\tilde{E}(\mu, \mu_0)}{dt} = \\ \left(P_0 + \frac{\alpha(\mu)}{2\pi} R \right) \left[\left(1 - \frac{\alpha(\mu)}{2\pi} C \right) \tilde{E} \right] . \end{aligned} \quad (\text{B.14})$$

Multiplying both sides on the left by $(1 + \alpha(\mu)/2\pi C)$, and neglecting higher-order terms consistently, we get

$$\frac{d\tilde{E}(\mu, \mu_0)}{dt} = \left(P_0 + \frac{\alpha(\mu)}{2\pi} \left[R + CP_0 - P_0C - \frac{b_0}{2}C \right] \right) \tilde{E}(\mu, \mu_0) . \quad (\text{B.15})$$

As a last point, we need to specialize our result to the standard cases in which one separates singlet and non-singlet component in the evolution equation. It is clear that for the non-singlet components we have $C_{\text{NS}} = -d_1$, and the commutator term is zero. For the gluon and singlet components, the C_{S} matrix has the form

$$C_{\text{S}} = \begin{vmatrix} C_{gg} & C_{gq} \\ C_{qg} & C_{qq} \end{vmatrix} = \begin{vmatrix} 0 & 0 \\ 0 & -d_1 \end{vmatrix} . \quad (\text{B.16})$$

Next we describe how to implement the scheme change in the short- distance partonic kernel cross sections, written in the notation of [9]. The Born cross section has the form (see also eq. (2.5))

$$\sigma_b = \int dx_3 \int_{VW/x_3}^{1-(1-V)/x_3} dv F_0(v, x_3) \mathcal{L}(x_1, x_2) D(x_3)/x_3^2 , \quad (\text{B.17})$$

where

$$x_1 = \frac{VW}{vx_3} , \quad x_2 = \frac{1-V}{(1-v)x_3} . \quad (\text{B.18})$$

Observe that the limits on v imply a limit on x_3

$$\frac{VW}{x_3} < 1 - \frac{1-V}{x_3} \rightarrow x_3 > 1 - V + VW . \quad (\text{B.19})$$

We now introduce a scheme transformation for the fragmentation function

$$D(x_3) = \tilde{D}(x_3) + \int dy dz \delta(x_3 - yz) p(y) \tilde{D}(z) . \quad (\text{B.20})$$

The second term of eq. (B.20), combined with the Born term in eq. (B.17), gives rise to a correction to the next-to-leading contribution. We wish to cast this correction in the same form as the next-to-leading term in eq. (2.5), so as to implement it easily in the numerical code.

The following change of variables

$$w' = \frac{vy}{vy + (1-y)} , \quad v' = 1 - y(1-v) , \quad (\text{B.21})$$

with the inverse

$$y = 1 - v'(1 - w') , \quad v = \frac{v'w'}{v'w' + 1 - v'} , \quad (\text{B.22})$$

maps the unit square onto the unit square, thus the integration range $0 < y < 1, 0 < v < 1$ is equivalent to the range $0 < w' < 1, 0 < v' < 1$. The determinant is

$$dv dy = dv' dw' \frac{v'}{v'w' + 1 - v'} \quad (\text{B.23})$$

and

$$x_1 = \frac{VW}{v'w'z} , \quad x_2 = \frac{1-V}{(1-v')z} . \quad (\text{B.24})$$

The limits on v imply

$$\begin{aligned} 1 - V + VW &< z < 1 , \\ \frac{VW}{z} &< v' < 1 - \frac{1-V}{z} \\ \frac{VW}{zv'} &< w' < 1 . \end{aligned} \quad (\text{B.25})$$

In terms of the new variables the cross section becomes

$$\sigma_b = \int_{1-V+VW}^1 dx_3 \int_{VW/x_3}^{1-(1-V)/x_3} dv F_0(v, x_3) \mathcal{L}(x_1, x_2) \tilde{D}(x_3)/x_3^2 + \delta\sigma , \quad (\text{B.26})$$

where

$$\begin{aligned} \delta\sigma &= \int_{1-V+VW}^1 dz \int_{VW/z}^{1-(1-V)/z} dv' \int_{VW/(zv')}^1 dw' \\ &\quad \frac{v'}{(v'w' + 1 - v')^3} F_0(v, yz) \mathcal{L}(x_1, x_2) p(y) \tilde{D}(z)/z^2 . \end{aligned} \quad (\text{B.27})$$

The structure of this equation coincides with that of the next-to-leading term in eq. (2.5), as desired.

Since $p(y)$ is a distribution at $y = 1$, it is convenient to rewrite the above formula as

$$\begin{aligned} \delta\sigma = & \int_{1-V+VW}^1 dz \int_{VW/z}^{1-(1-V)/z} dv' \left\{ \int_{VW/(zv')}^1 dw' p(y) \right. \\ & \left[\frac{v'}{(v'w' + 1 - v')^3} F_0(v, yz) \mathcal{L}(x_1, x_2) - v' F_0(v', z) \mathcal{L}(x'_1, x'_2) \right] \tilde{D}(z)/z^2 \\ & + \int_{1-V+VW}^1 dz \int_{VW/z}^{1-(1-V)/z} dv' v' F_0(v', z) \mathcal{L}(x'_1, x'_2) \tilde{D}(z)/z^2 \\ & \left. \times \int_{VW/(zv')}^1 dw' p(y) \right\}, \end{aligned} \quad (\text{B.28})$$

where

$$x'_{1/2} = x_{1/2}|_{w'=1}. \quad (\text{B.29})$$

In the DL scheme

$$p(y) = \frac{\alpha C_f}{2\pi} \left[\frac{1+y^2}{1-y} (-1 - 2\log(1-y)) \right]_+. \quad (\text{B.30})$$

Using the fact that

$$\int_0^1 p(y) dy = 0, \quad (\text{B.31})$$

we have

$$\int_{VW/(zv')}^1 dw' p(y) = - \int_{-(1-v')/v'}^{VW/(zv')} p(v'w' + 1 - v') dw' = -\frac{1}{v'} \int_0^{1-v'+VW/z} p(y) dy, \quad (\text{B.32})$$

where

$$\int_0^y p(y) dy = \frac{\alpha C_f}{2\pi} (\log(1-y)(y^2 + 2y - 1) - 2y + 2\log^2(1-y)). \quad (\text{B.33})$$

References

- [1] P. Nason, S. Dawson and R. K. Ellis, *Nucl. Phys.* **B303**(1988)607.
- [2] P. Nason, S. Dawson and R. K. Ellis, *Nucl. Phys.* **B327**(1989)49; erratum *ibid.* **B335**(1990)260.

- [3] W. Beenakker, H. Kuijf, W.L. van Neerven and J. Smith, *Phys. Rev.* **D40**(1989)54.
- [4] W. Beenakker, W.L. van Neerven, R. Meng, G.A. Schuler and J. Smith, *Nucl. Phys.* **B351**(1991)507.
- [5] M. Cacciari and M. Greco, *Nucl. Phys.* **B421**(1994)530, [hep-ph/9311260](#).
- [6] F.I. Olness, R.J. Scalise and Wu-Ki Tung, preprint CTEQ-616, [hep-ph/9712494](#).
- [7] M.A.G. Aivazis, J.C. Collins, F.I. Olness and W.-K. Tung, *Phys. Rev.* **D50**(1994)3102.
- [8] B. Mele and P. Nason, *Nucl. Phys.* **B361**(1991)626.
- [9] F. Aversa, P. Chiappetta, M. Greco and J.Ph. Guillet, *Nucl. Phys.* **B327**(1989)105.
- [10] P. Aurenche, R. Baier, A. Douiri, M. Fontannaz and D. Schiff, *Nucl. Phys.* **B286**(1987)553.
- [11] P. Aurenche, R. Baier, A. Douiri, M. Fontannaz and D. Schiff, *Z. Phys.* **C29**(1985)423;
L.E. Gordon, *Phys. Rev.* **D50**(1994)6753.
- [12] M. Cacciari and M. Greco, *Z. Phys.* **C69**(1996)459.
- [13] M. Cacciari, M. Greco, M. Krämer, G. Kramer, B. Kniehl and M. Spira, *Nucl. Phys.* **B466**(1996)173.
- [14] R.K. Ellis and P. Nason, *Nucl. Phys.* **B312**(1989)551;
J. Smith and W.L. van Neerven, *Nucl. Phys.* **B374**(1992)36.
- [15] M. Krämer, J. Zunft, J. Steegborn and P.M. Zerwas, *Phys. Lett.* **B348**(1995)657.
- [16] J. Collins, F. Wilczek and A. Zee, *Phys. Rev.* **D18**(1978)242.
- [17] J.C. Collins and Wu-Ki Tung, *Nucl. Phys.* **B278**(1986)934.
- [18] M. Cacciari and M. Greco, *Phys. Rev.* **D55**(1997)7134, [hep-ph/9702389](#).

- [19] G. Colangelo and P. Nason, *Phys. Lett.* **B285**(1992)167;
S. Frixione, M.L. Mangano, P. Nason and G. Ridolfi, “Heavy-Quark Production”, [hep-ph/9702287](#), published in “Heavy Flavours II”, eds. A.J. Buras and M. Lindner, Advanced Series on Directions in High Energy Physics, (World Scientific Publishing Co., Singapore).
- [20] W. Furmanski and R. Petronzio, *Z. Phys.* **C11**(1982)293.